

## Research Article

# Simultaneous Recording of ICG and ECG Using Z-RPI Device with Minimum Number of Electrodes

Abdelakram Hafid <sup>1</sup>, Sara Benouar,<sup>1</sup> Malika Kedir-Talha,<sup>1</sup> Mokhtar Attari,<sup>1</sup>  
and Fernando Seoane<sup>2,3,4</sup>

<sup>1</sup>Laboratory of Instrumentation, University of Sciences and Technology Houari Boumediene, Algiers, Algeria

<sup>2</sup>Swedish School of Textiles, University of Borås, 50190 Borås, Sweden

<sup>3</sup>The Department for Clinical Science, Intervention and Technology, Karolinska Institutet, 14186 Stockholm, Sweden

<sup>4</sup>Department Biomedical Engineering, Karolinska University Hospital, 14186 Stockholm, Sweden

Correspondence should be addressed to Abdelakram Hafid; [abdelakram.hafid@gmail.com](mailto:abdelakram.hafid@gmail.com)

Received 30 June 2018; Revised 28 September 2018; Accepted 1 October 2018; Published 29 November 2018

Guest Editor: David Naranjo-Hernández

Copyright © 2018 Abdelakram Hafid et al. This is an open access article distributed under the Creative Commons Attribution License, which permits unrestricted use, distribution, and reproduction in any medium, provided the original work is properly cited.

Impedance cardiography (ICG) is a noninvasive method for monitoring mechanical function of the heart with the use of electrical bioimpedance measurements. This paper presents the feasibility of recording an ICG signal simultaneously with electrocardiogram signal (ECG) using the same electrodes for both measurements, for a total of five electrodes rather than eight electrodes. The device used is the Z-RPI. The results present good performance and show waveforms presenting high similarity with the different signals reported using different electrodes for acquisition; the heart rate values were calculated and they present accurate evaluation between the ECG and ICG heart rates. The hemodynamics and cardiac parameter results present similitude with the physiological parameters for healthy people reported in the literature. The possibility of reducing number of electrodes used for ICG measurement is an encouraging step to enabling wearable and personal health monitoring solutions.

## 1. Introduction

An estimated 17.5 million deaths per year are attributed to cardiac diseases. According to WHO [1], people with cardiovascular diseases (CVDs) require an early and pertinent diagnosis to receive the best treatment [2].

Electrical bioimpedance (EBI) is a sensing technology that has been used for several decades for various applications [3], utilizing different measurement techniques, e.g., segmental and/or total body [4], spectroscopy [5, 6], tomography [7], and impedance plethysmography [8] with its most common application which is impedance cardiography (ICG). Using a single channel with single frequency continuously, the ICG was introduced as a noninvasive method and its waveform has been used for the assessment of certain hemodynamic parameters describing the mechanical function of the heart like the cardiac output (CO), stroke volume (SV), and systolic time intervals, e.g., left ventricular ejection

time (LVET noted also ET), preejection period (PEP), and systolic time ratio (STR) [9–11].

An ICG recording is obtained using a specific electrode configuration, the electrodes are placed on the surface of the upper torso, and the EBI is measured across the thorax with the 4-electrode measurement technique from the neck to the abdomen [12]. The measured variation of the impedance ( $Z$ ) is mainly due to the cardiac activity; it is noted  $\Delta Z$ ; the  $dZ/dt$  waveform is obtained from the first derivative of the  $\Delta Z$  signal, and it is characterized by seven typical characteristic points which are related to cardiodynamics [10, 13].

Electrocardiography (ECG) is a relatively inexpensive technique that allows simple and noninvasive monitoring of the electrical activity of the heart. The action potentials generated during the activity of the heart can be collected by electrodes placed on the surface of the skin. The location of these electrodes is chosen to explore the lead II of the heart electric field.

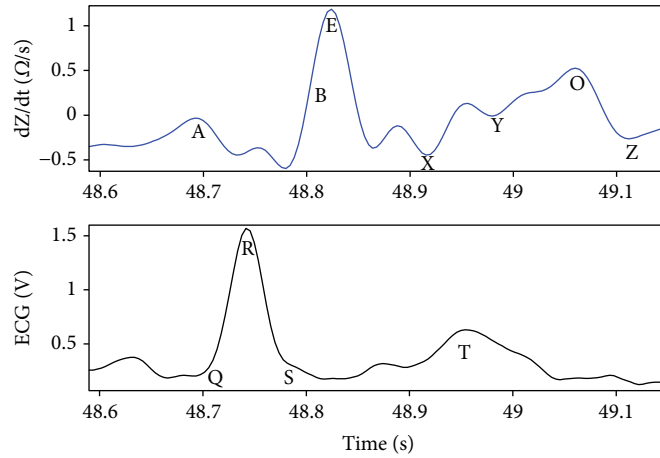


FIGURE 1: Pattern of the ICG and ECG signals simultaneously.

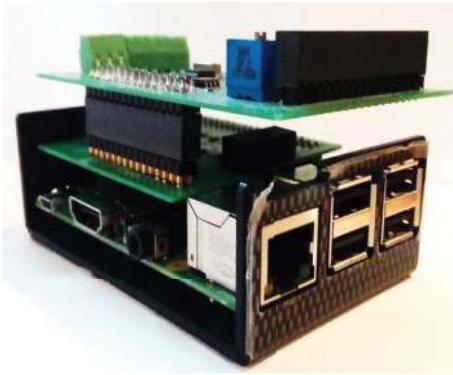


FIGURE 2: Z-RPI prototype.

Cardiogenic bioelectrical activity is commonly called ECG lead or derivation. Each ECG derivation is defined by a specific label and a precise electrode placement according to [14]; there are different derivations used to measure the ECG signal; each of them has a number and precise electrode locations, such as standard bipolar peripheral derivations, unipolar peripheral derivations, and precipitation unipolar derivations [15].

ECG-based heart rate calculation involves the step of detecting the *R* wave of the QRS complex. The most common method for detecting the *R* wave is the Pan-Tompkins algorithm [16–18].

Development of personalized health (p-health) solutions and advances in smart textiles and textile manufacturing has allowed new developments of wearable measurement systems targeting fitness and even home-care but often they have been limited to biopotential recordings [19, 20]. Recent advances in microelectronics have produced system-on-chip (SoC) solutions for biopotential and bioimpedance measurements, and most of them have been successfully tested in several EBI applications [21–25]. Thus, we can confirm that their availability and accessibility have indeed fostered research and development activities targeting p-health monitoring applications based on different embedded

electronic wearable measurement systems and patch technology [23, 26–28].

Thus, for performing ICG and ECG measurements, using two different electrodes' placement to make a simultaneous record is generally the method that is used.

ICG waveforms together with ECG waveforms as presented in Figure 1 are often used to calculate and assess the specific hemodynamic parameters mentioned above [9, 10].

In this paper, we present a measurement system for the acquisition of ICG and one-lead ECG signal simultaneously using the same electrodes for both measurements. The Pan-Thompkins algorithm is used for ECG analysis, and the ensemble average method is applied to assess hemodynamic parameters of the ICG signal.

## 2. Methods

**2.1. Z-RPI Device.** The developed ICG recording device used in this work showed in Figure 2 named Z-RPI is a custom-made device that can simultaneously record ECG and ICG. It combines two system-on-chip (SoC) solutions, which are ADAS1000 and AD5933 from Analog Devices combined with additional electronics to have a complete EBI and ECG measurement modules, with the Raspberry PI3 card. It also includes an impedance calibration system, Bluetooth wireless communication, a power management circuit, and a 2500 mAh LiPo battery as power supply with 5 hours of autonomy [24], in its original operation mode, for recording ICG and ECG.

**2.2. Experimental Measurement Setup.** The regular configuration of the Z-RPI device uses 8 electrodes: 4 electrodes for measuring ICG, in which the electrodes are placed according to the Sramek configuration (two electrodes on the right lateral part of the neck and two on the left side of the thorax) [12]; 3 electrodes for ECG; and 1 electrode for the RLD circuitry, placed in the peripheral extremities (hand and leg) for the ECG [24].

In this work, the configuration of the Z-RPI device has been modified, especially for the ADAS1000 part, which has been moved from a 3-lead ECG recording configuration

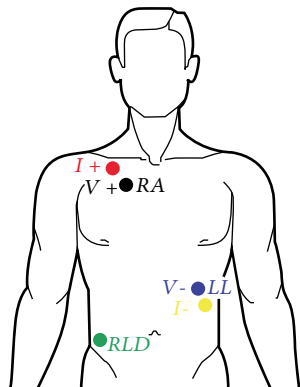


FIGURE 3: Placement of electrodes for ECG/ICG measurement.

TABLE 1: Mean and the SD of anthropomorphic data of volunteers.

Gender	<i>N</i>	Height (cm)	Weight (kg)	Age (years)
Male	7	180 ± 7	81 ± 9	31 ± 13

to a single-lead recording. As we do not have a golden standard for the placement of the ICG electrodes, we chose to place two electrodes on the right lateral part of the upper torso and two electrodes on the left side of the thorax, on the upper abdomen part, and the RLD electrode is placed at the right side of the waist.

As we use a tetrapolar configuration for performing ICG measurement, the placement configuration of the electrodes has been chosen to have the inner ICG electrode (V+ and V-) in the same position as the RA and LL spot for the ECG measurement. In this way, the ECG shielded cables were connected to them (V+ with RA and V- with LL) for performing simultaneously the ICG measurement and ECG lead II measurement.

Figure 3 shows the five spots for the placement of the 3M repositionable Ag/AgCl gel electrodes used for performing the ICG recording [12] and one-lead ECG; the shared voltage-sensing electrodes are marked with V in black and blue, and the current injecting electrodes are the outer ones, indicated with I in red and yellow.

The experimental evaluation was performed at the Laboratory of Instrumentation at the University of Science and Technology Houari Boumediene, Algeria, on seven healthy volunteers (see Table 1). The recordings in the experiment were obtained according to the procedure previously used in [24] and approved by the ethical approval nr 11-274 granted by the regional Ethical Vetting Board in Gothenburg including the use of an informed consent form.

The ICG measurement is obtained using an injecting sinusoidal current of 70 kHz and 133  $\mu$ A [24], and 280 Hz sampling frequency acquisition was used for both ICG and ECG recording. The measurement sessions lasted for at least 60 seconds while the subjects remained in sitting position keeping a shallow breathing paced at 10 breaths per minute.

**2.3. Measurement Data Analysis.** The recorded thoracic measurements were processed and analyzed on the PC using a

customized program running MATLAB 2015 scripts [24]; high-frequency information is removed applying a low-pass filter with frequency cut at 13 Hz. Since the acquired impedance  $\Delta Z$  includes both cardiac and respiration components, knowing that the respiration is present in the band of 0.05–0.3 Hz, approximately, a bandpass filter was designed in a 20th-order FIR filter with  $f_c = 0.7$ –7 Hz. Therefore, the respiration components attenuated a minimum of –6 dB, and the different characterizing parameters and time interval values of the ICG and ECG signal were extracted. More details are present elsewhere in [24].

**2.4. Hemodynamic Parameter Calculation.** The Pan-Tompkins algorithm [17] was used for detecting the R peak in the ECG recording. Once the R peak is detected, the Q point is extracted from the QRS complex of the ECG signal. The Q point is the minimum before the R peak; it was calculated by subtracting a fixed value of 40 ms from the time of the R wave [29]. Using the R and Q waves, the heart rate (HR) and the PEP are calculated, respectively.

The  $\Delta Z$  and  $dZ/dt$  signals obtained from the ICG recording were analyzed to obtain the different ICG parameters, using the ensemble average method [30, 31]; the  $dZ/dt_{\max}$  (*E* point) is the peak of the first derivative of the transthoracic impedance variation in  $\Omega/s$  [32]; this later is triggered by the R peaks of the ECG signals. The heart rate of the ICG signal was calculated from the *E* peaks acquired. The LVET interval is calculated as the distance between *B* and *X* point of the ICG signal. Then, SV and CO are calculated according to (1) and (2), respectively, as presented in [24].

$$SV = V_C \sqrt{\frac{dZ(t)/dt_{\max}}{Z_0}} ET, \quad (1)$$

$$CO = SV \times HR. \quad (2)$$

### 3. Results

More than 2700 seconds of recordings were obtained, containing more than 3000 ICG and ECG complexes, similar to the ones plotted in Figure 4. Figure 4(a) shows the  $\Delta Z$ , Figure 4(b) shows the  $dZ/dt$ , and Figure 4(c) shows the ECG.

Figure 5 presents the averaged complexes ICG thin trace in ( $\Omega/s$ ) and ECG coarse trace in (V) obtained from 60 s of recordings of the healthy volunteer HV1.

Table 2 presents the descriptive statistics (mean  $\pm$  SD) for the characterizing parameters and time interval values, calculated from the ICG/ECG recordings obtained for each volunteer.

Figure 6 presents two averaged ICG complexes produced with the recordings obtained with the 2 different electrode configurations. The recordings obtained with the 5-electrode configuration, continuous trace, show a remarkable minimum between the *A* and *E* waves of the ICG complex, minimum significantly more pronounced than the minimum obtained with the 8-electrode configuration.

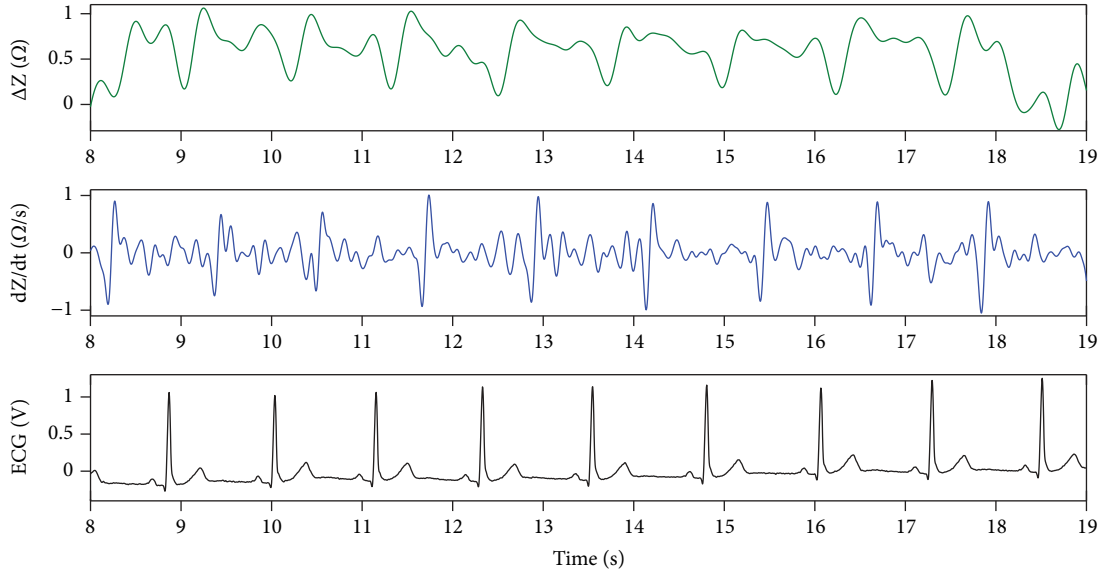


FIGURE 4:  $\Delta Z$ ,  $dZ/dt$ , and ECG recorded from one volunteer.

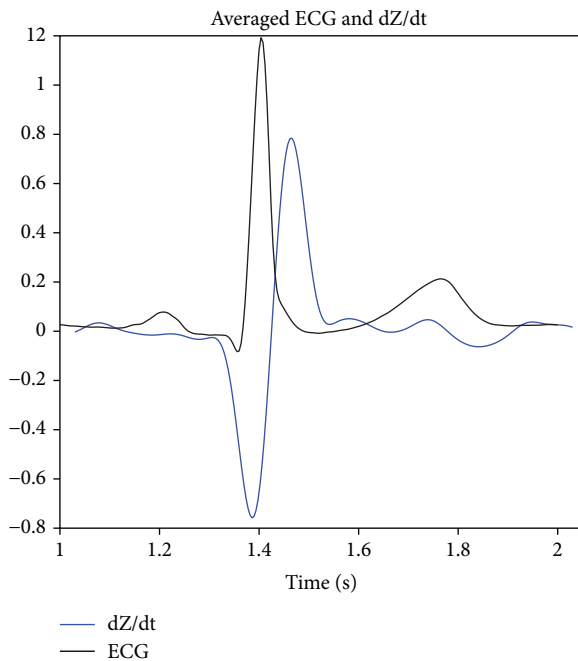


FIGURE 5: Averaged ICG and ECG signal.

#### 4. Discussion

The purpose of this paper was to evaluate the feasibility of obtaining simultaneously both the ICG and 1-lead ECG, lead II, recordings using the same electrodes for voltage sensing plus one electrode for right leg driven.

The performed measurements sharing the sensing electrodes allowed us to obtain a clean raw ECG,  $\Delta Z$ , and  $dZ/dt$  recordings. However, as showed in Figure 6, the ICG complex obtained with 5 electrodes produces a much denoted minimum than in the recordings obtained with 8

electrodes. Such denoted minimum between the A and E waves appears in all volunteers and can be observed also in the recording showed in Figure 4. This change in the waveform most likely occurs due to the fact that the placement of the electrodes is slightly different between the 5-electrode and 8-electrode configuration [33], where the upper electrode from the neck is placed in the upper section of the torso as shown in Figure 3.

Previously, researchers have raised concerns about problems in experiments, to obtain a straightforward and reliable detection of ICG characteristic points and hemodynamic parameter calculation, especially in automated processing [9, 34–36]. Thus, such denoted minimum is very useful because it allows developing an algorithm for synchronization of ICG complex for the averaging method [30, 31].

Nevertheless, the waveforms obtained using the 5 electrodes as expected exhibit a denoted similarity to other standard ECG and ICG measurements reported elsewhere in the literature [10, 27, 37].

With the exception of the value for HR obtained from ECG, the rest of the hemodynamic and cardiac parameters, SV, CO, and time intervals as the ET and the PEP are obtained from the ICG measurement. The obtained values show certain variability, but such variability can be found between different commercial ICG recorders as reported in [10, 38].

Moreover, given that different electrode configurations as presented in the literature [12, 39–42] yield different results showing also certain dependency to the method use in the analysis [10, 38], we cannot reject the hypothesis that part of the observed variability actually comes from the placement of electrodes. However, the values obtained for the HR and ICG parameters are equivalent and present similar values to hemodynamic parameters obtained from healthy people and reported in the literature [10, 24, 43].

TABLE 2: Cardiac and hemodynamic parameters calculated from the acquired ECG and ICG (mean  $\pm$  SD).

Parameters	HV1	HV2	HV3	HV4	HV5	HV6	HV7
$Z_0$ ( $\Omega$ )	$37.61 \pm 6.2$	$36.84 \pm 6.5$	$37.12 \pm 4.7$	$48.39 \pm 6.9$	$45.94 \pm 4.7$	$27.17 \pm 8.7$	$69.38 \pm 1.7$
$dZ/dt_{\max}$ ( $\Omega/s$ )	$1.03 \pm 0.07$	$1.10 \pm 0.14$	$1.37 \pm 0.16$	$1.36 \pm 0.1$	$1.55 \pm 0.11$	$1.22 \pm 0.06$	$1.42 \pm 0.2$
ET (ms)	$211 \pm 13$	$286 \pm 5$	$319 \pm 13$	$183 \pm 1$	$165 \pm 11$	$210 \pm 4$	$184 \pm 7$
SV (ml)	$54 \pm 3$	$52 \pm 3$	$83 \pm 7$	$43 \pm 2$	$42 \pm 1$	$68 \pm 14$	$46 \pm 4$
CO (l/min)	$4.45 \pm 0.26$	$5.04 \pm 0.16$	$4.29 \pm 0.4$	$3.08 \pm 0.15$	$3.02 \pm 0.1$	$4.67 \pm 0.65$	$2.52 \pm 0.06$
PEP (ms)	$87 \pm 19$	$55 \pm 8$	$90 \pm 6$	$92 \pm 33$	$81 \pm 22$	$81 \pm 17$	$90 \pm 4$
HR <sub>ECG</sub> (bpm)	$82 \pm 1$	$97 \pm 2$	$51 \pm 1$	$71 \pm 2$	$71 \pm 1$	$68 \pm 7$	$54 \pm 4$
HR <sub>Z</sub> (bpm)	$82 \pm 1$	$97 \pm 2$	$50 \pm 1$	$70 \pm 2$	$69 \pm 1$	$67 \pm 5$	$54 \pm 5$

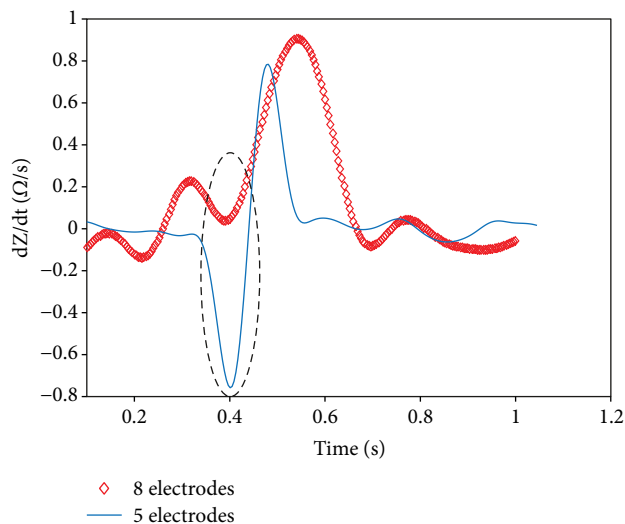


FIGURE 6: Averaged signal for both 5 electrode- vs. 8-electrode configuration.

Thus, this work reinforces the pavement towards wearable applications for engineering, educational, and/or research purposes, in a way that was originally paved by the work done within the HeartCycle project with the wearable impedance cardiographer named IMPACT T-shirt [23] where 8 electrodes were used.

In this paper, one expected confers with such measurement configuration (where the voltage electrodes acquired both the cardiogenic biopotential and the voltage caused by the current injection) would be a certain kind of cross talking of some kind that would create interferences between the different sensing modalities. The close inspection of the recording shows recordings completely free from artifacts caused by interferences between the ICG and the ECG. Consequently, we can assert that the ICG/ECG recordings have been obtained satisfactorily sharing the biopotential electrodes.

Overall, after the evaluation of the obtained recordings, the descriptive statistics of the hemodynamic parameters show a remarkable performance, where the standard deviation is considerably low. In addition, the concordance of the heart rate values between ICG and ECG measurements is obtained.

## 5. Conclusion

The evaluation results show that the affordable Z-RPI device functions effectively and accurately when performing ECG and ICG simultaneously using only 5 electrodes.

Such successful implementation of the Z-RPI with a reduced number of electrodes facilitates the use of sensorized garments with integrated textile electrodes [27, 43] for wearable and p-health monitoring applications of transthoracic bioimpedance.

Thus, this will also enhance the accuracy of the detection of characteristic points and the calculation of hemodynamic parameters.

With the configuration of electrodes that we presented with the Z-RPI device, we had shown the feasibility of developing an affordable full impedance cardiographer and one-lead electrocardiography device with minimum electrode number. The configuration of electrodes that we are offering in this paper will allow us to go for a comfortable T-shirt that does not have any electrodes or turtleneck around the neck, since the electrodes are placed slightly down to the neck. Thus, we aim to optimize the flexibility and maneuverability and to have greater freedom of action when using a textile garment with a complete affordable device, for the perspective of developing in the future wearable device for p-health or sport effort application.

## Data Availability

The data used to support the findings of this study are available from the corresponding author upon request.

## Conflicts of Interest

Fernando Seoane is cofounder of Z-Health Technologies AB; neither proprietary technology nor methods of Z-Health Technologies have been used in this work.

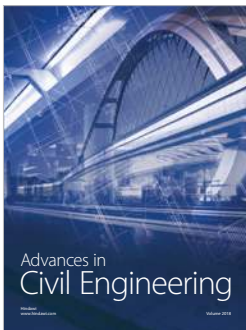
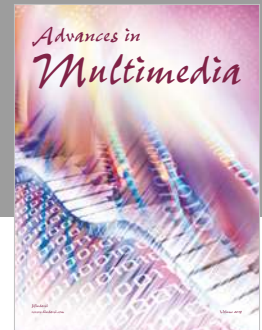
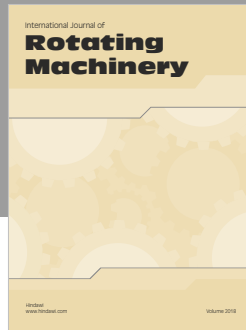
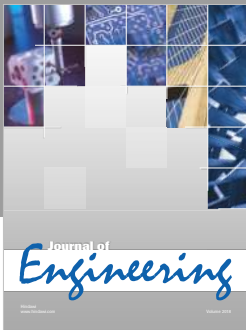
## Acknowledgments

The authors would like to thank the research group Textile and Wearable Sensing for p-Health Solutions, at Borås University. This work was supported by the Ministère de l'Enseignement Supérieur et de la Recherche Scientifique (MESRS), Algerian Government.

## References

- [1] World Health Organization, *Cardiovascular Diseases (CVDs)*, Media centre, 2016.
- [2] S. Said and G. T. Hernandez, "The link between chronic kidney disease and cardiovascular disease," *Journal of Nephro-pathology*, vol. 3, no. 3, pp. 99–104, 2014.
- [3] T. K. Bera, "Bioelectrical impedance methods for noninvasive health monitoring: a review," *Journal of Medical Engineering*, vol. 2014, 28 pages, 2014.
- [4] U. G. Kyle, I. Bosaeus, A. D. de Lorenzo et al., "Bioelectrical impedance analysis—part I: review of principles and methods," *Clinical Nutrition*, vol. 23, no. 5, pp. 1226–1243, 2004.
- [5] J. C. Marquez, F. Seoane, E. Välimäki, and K. Lindcrantz, "Comparison of dry-textile electrodes for electrical bioimpedance spectroscopy measurements," *Journal of Physics: Conference Series*, vol. 224, article 012140, 2010.
- [6] F. Seoane, S. Reza Atefi, J. Tomner, K. Kostulas, and K. Lindcrantz, "Electrical bioimpedance spectroscopy on acute unilateral stroke patients: initial observations regarding differences between sides," *BioMed Research International*, vol. 2015, 12 pages, 2015.
- [7] R. V. Davalos, D. M. Otten, L. M. Mir, and B. Rubinsky, "Electrical impedance tomography for imaging tissue electroporation," *IEEE Transactions on Biomedical Engineering*, vol. 51, no. 5, pp. 761–767, 2004.
- [8] J. Nyboer, M. M. Kreider, and L. Hannapel, "Electrical impedance plethysmography," *Circulation*, vol. 2, no. 6, pp. 811–821, 1950.
- [9] A. Sherwood, M. T. Allen, J. Fahrenberg, R. M. Kelsey, W. R. Lovallo, and L. J. P. Doornen, "Methodological guidelines for impedance cardiography," *Psychophysiology*, vol. 27, no. 1, pp. 1–23, 1990.
- [10] G. Cybulski, "Ambulatory impedance cardiography," in *Ambulatory Impedance Cardiography. Lecture Notes in Electrical Engineering*, vol. 76, pp. 39–56, Springer, Berlin, Heidelberg, 2011.
- [11] D. P. Bernstein, I. C. Henry, M. J. Banet, and T. Dittrich, "Stroke volume obtained by electrical interrogation of the brachial artery: transbrachial electrical bioimpedance velocimetry," *Physiological Measurement*, vol. 33, no. 4, pp. 629–649, 2012.
- [12] H. H. Woltjer, B. J. M. van der Meer, H. J. Bogaard, and P. M. J. M. de Vries, "Comparison between spot and band electrodes and between two equations for calculations of stroke volume by means of impedance cardiography," *Medical and Biological Engineering and Computing*, vol. 33, no. 3, pp. 330–334, 1995.
- [13] Z. Lababidi, D. A. Ehmke, R. E. Durnin, P. E. Leaverton, and R. M. Lauer, "The first derivative thoracic impedance cardiogram," *Circulation*, vol. 41, no. 4, pp. 651–658, 1970.
- [14] R. J. Prineas, R. S. Crow, and Z.-M. Zhang, *The Minnesota Code Manual of Electrocardiographic Findings*, Springer Science & Business Media, 2009.
- [15] J. D. Dominique Farge, A. Ducros, and C. Neuzillet, "Le livre de sémiologie médicale," 2012, <http://www.e-semio.org/Derivation-ECG-frontales>.
- [16] N. Debbabi, S. El Asmi, and H. Arfa, "Correction of ECG baseline wander application to the Pan & Tompkins QRS detection algorithm," in *2010 5th International Symposium on I/V Communications and Mobile Network (ISVC)*, pp. 1–4, Rabat, Morocco, September–October 2010.
- [17] J. Pan and W. J. Tompkins, "A real-time QRS detection algorithm," *IEEE Transactions on Biomedical Engineering*, vol. BME-32, no. 3, pp. 230–236, 1985.
- [18] H. Zairi, M. Kedir-Talha, S. Benouar, and A. Ait-Amer, "Intelligent system for detecting cardiac arrhythmia on FPGA," in *2014 5th International Conference on Information and Communication Systems (ICICS)*, pp. 1–5, Irbid, Jordan, April 2014.
- [19] N. Meziane, J. G. Webster, M. Attari, and A. J. Nimunkar, "Dry electrodes for electrocardiography," *Physiological Measurement*, vol. 34, no. 9, pp. R47–R69, 2013.
- [20] N. Meziane, S. Yang, M. Shokouejad, J. G. Webster, M. Attari, and H. Eren, "Simultaneous comparison of 1 gel with 4 dry electrode types for electrocardiography," *Physiological Measurement*, vol. 36, no. 3, pp. 513–529, 2015.
- [21] R. Harder, A. Diedrich, J. S. Whitfield, M. S. Buchowski, J. B. Pietsch, and F. J. Baudenbacher, "Smart multi-frequency bioelectrical impedance spectrometer for BIA and BIVA applications," *IEEE Transactions on Biomedical Circuits and Systems*, vol. 10, no. 4, pp. 912–919, 2016.
- [22] F. Abtahi, B. Aslami, I. Boujabir, F. Seoane, and K. Lindcrantz, "An affordable ECG and respiration monitoring system based on Raspberry PI and ADAS1000: first step towards homecare applications," *16th Nordic-Baltic Conference on Biomedical Engineering. IFMBE Proceedings*, vol. 48, H. Mindedal and M. Persson, Eds., pp. 5–8, Springer, Cham, 2015.
- [23] M. Ulbrich, J. Mühlsteff, A. Sipilä et al., "The IMPACT shirt: textile integrated and portable impedance cardiography," *Physiological Measurement*, vol. 35, no. 6, pp. 1181–1196, 2014.
- [24] A. Hafid, S. Benouar, M. Kedir-Talha, F. Abtahi, M. Attari, and F. Seoane, "Full impedance cardiography measurement device using Raspberry PI3 and system-on-chip biomedical instrumentation solutions," *IEEE Journal of Biomedical and Health Informatics*, vol. 22, no. 6, pp. 1883–1894, 2018.
- [25] S. Weyer, T. Menden, L. Leicht, S. Leonhardt, and T. Wartzek, "Development of a wearable multi-frequency impedance cardiography device," *Journal of Medical Engineering & Technology*, vol. 39, no. 2, pp. 131–137, 2015.
- [26] J. M. M. Ulbrich, H. Reiter, C. Meyer, and S. Leonhardt, "Wearable solutions using bioimpedance for cardiac monitoring," in *Recent Advances in Ambient Assisted Living-Bridging Assistive Technologies, E-Health and Personalized Health Care*, vol. 20, pp. 30–44, IOS Press, 2015.
- [27] J. C. M. Ruiz, M. Rempfler, F. Seoane, and K. Lindcrantz, "Textrode-enabled transthoracic electrical bioimpedance measurements-towards wearable applications of impedance cardiography," *Journal of Electrical Bioimpedance*, vol. 4, no. 1, pp. 45–50, 2013.
- [28] M. J. Liebo, R. P. Katra, N. Chakravarthy, I. Libbus, and W. H. W. Tang, "Noninvasive wireless bioimpedance monitoring tracks patients with healthcare utilization following discharge from acute decompensated heart failure: results from the ACUTE pilot study," *Journal of Cardiac Failure*, vol. 19, no. 8, pp. S88–S89, 2013.
- [29] R. van Lien, N. M. Schutte, J. H. Meijer, and E. J. C. de Geus, "Estimated preejection period (PEP) based on the detection of the R-wave and dZ/dt-min peaks does not adequately reflect the actual PEP across a wide range of laboratory and ambulatory conditions," *International Journal of Psychophysiology*, vol. 87, no. 1, pp. 60–69, 2013.

- [30] R. M. Kelsey and W. Guethlein, "An evaluation of the ensemble averaged impedance cardiogram," *Psychophysiology*, vol. 27, no. 1, pp. 24–33, 1990.
- [31] H. Riese, P. F. C. Groot, M. van den Berg et al., "Large-scale ensemble averaging of ambulatory impedance cardiograms," *Behavior Research Methods, Instruments, & Computers*, vol. 35, no. 3, pp. 467–477, 2003.
- [32] W. G. Kubicek, J. Kottke, M. U. Ramos et al., "The Minnesota impedance cardiograph-theory and applications," *Bio-Medical Engineering*, vol. 9, no. 9, pp. 410–416, 1974.
- [33] K. Sakamoto, K. Muto, H. Kanai, and M. Iizuka, "Problems of impedance cardiography," *Medical and Biological Engineering and Computing*, vol. 17, no. 6, pp. 697–709, 1979.
- [34] A. P. DeMarzo and R. M. Lang, "A new algorithm for improved detection of aortic valve opening by impedance cardiography," in *Computers in Cardiology 1996*, pp. 373–376, Indianapolis, IN, USA, September 1996.
- [35] D. L. Lozano, G. Norman, D. Knox et al., "Where to B in  $dZ/dt$ ," *Psychophysiology*, vol. 44, no. 1, pp. 113–119, 2007.
- [36] J. H. Meijer, S. Boesveldt, E. Elbertse, and H. W. Berendse, "Method to measure autonomic control of cardiac function using time interval parameters from impedance cardiography," *Physiological Measurement*, vol. 29, no. 6, pp. S383–S391, 2008.
- [37] J. Ferreira, F. Seoane, and K. Lindcrantz, "Portable bioimpedance monitor evaluation for continuous impedance measurements. Towards wearable plethysmography applications," in *2013 35th Annual International Conference of the IEEE Engineering in Medicine and Biology Society (EMBC)*, pp. 559–562, Osaka, Japan, July 2013.
- [38] P. Carvalho, R. P. Paiva, J. Henriques, M. Antunes, I. Quintal, and J. Muehlsteff, "Robust characteristic points for ICG-definition and comparative analysis," *Proceedings of the International Conference on Bio-inspired Systems and Signal Processing - Volume 1: BIOSIGNALS*, , pp. 161–168, Scienceand Technology Publications, Lda., Rome, Italy, 2011.
- [39] A. Ikarashi, M. Nogawa, S. Tanaka, and K.-i. Yamakoshi, "Experimental and numerical study on optimal spot-electrodes arrays in transthoracic electrical impedance cardiography," in *2007 29th Annual International Conference of the IEEE Engineering in Medicine and Biology Society*, pp. 4580–4583, Lyon, France, August 2007.
- [40] F. Hoekstra, E. Habers, T. W. J. Janssen, R. M. Verdaasdonk, and J. H. Meijer, "Relationship between the initial systolic time interval and RR-interval during an exercise stimulus measured with impedance cardiography," *Journal of Physics: Conference Series*, vol. 224, article 012117, 2010.
- [41] M. Qu, Y. Zhang, J. G. Webster, and W. J. Tompkins, "Motion artifact from spot and band electrodes during impedance cardiography," *IEEE Transactions on Biomedical Engineering*, vol. BME-33, no. 11, pp. 1029–1036, 1986.
- [42] E. Raaijmakers, T. J. C. Faes, H. G. Goovaerts, J. H. Meijer, P. M. J. M. de Vries, and R. M. Heethaar, "Thoracic geometry and its relation to electrical current distribution: consequences for electrode placement in electrical impedance cardiography," *Medical and Biological Engineering and Computing*, vol. 36, no. 5, pp. 592–597, 1998.
- [43] M. Ulbrich, *Non-Invasive Stroke Volume Assessment Using the Thoracic Electrical Bioimpedance:-Advances in Impedance Cardiography*, Shaker Verlag, 2016.



**Hindawi**

Submit your manuscripts at  
[www.hindawi.com](http://www.hindawi.com)

